

THERMODYNAMICAL AND MECHANICAL MODELLING ANALYSIS OF HIGH-SPEED TURBOMACHINE ROTORS

E. Saari, J. Backman, J. Larjola

Lappeenranta University of Technology, P.O. Box 20, 53851 Lappeenranta, Finland,
esa.saari@lut.fi

ABSTRACT

In this study it is considered problems appearing in the different applications of high-speed technology, having as the viewpoint the rotor structure. High-speed technology means a system, where the electric machine and the unit to be driven (turbine, compressor) are directly coupled to each other without a gear box, and where the speed of this common shaft is significantly higher than the synchronous speed of two pole electric machines connected to the 50/60 Hz network. The high power density is typical for rotors of high-speed machines. The objective of this study is to analyze the mechanical structure of the combined electric machine – turbo machine rotor in three points of view: 1) the literature review and summary of governing equations for design of high speed machines. 2) to reduce the heat sources and to improve the cooling of critical points. This involves the reduction of electric losses and the concentration of the losses to places favorable for cooling. 3) to analyze the strength of the fittings at assembly and at high speeds.

NOMENCLATURE

A	area [m ²]	n_s	rotational speed, [1/min]
A_c	linear current density [A/m]	p	number of pole pairs [pcs]
B_δ	flux density [T]	P	power [W]
C_f	friction coefficient [-]	q_m	mass flow [kg/s]
C	machine factor [-]	r	radius [m]
D	diameter of rotor [m]	s	gap length[m]
d_h	hydraulic diameter [m]	u_1	circumferential velocity [m/s]
f	frequency [Hz]	V	volume [m ³]
k_1	surface roughness coefficient [-]	Re	Reynolds number
k_2	velocity factor [-]	Nu	Nusselt number
k_w	winding factor[-]	Pr	Prandtl number
l	length [m]	ω	angular velocity [rad/s]
L	length of a rotor [m]	ρ	density[kg/m ³]
m	mass [kg]	δ	air gap [m]

INTRODUCTION

This study is based on the doctoral thesis by Saari, (2012), where from can be found more details of the subject. Software calculation has been completed by Ansys Workbench 14.0.

The development of high-speed technology (as defined in abstract) started in Finland thirty years ago. Rotor speed is typically over 10 000 rpm (Larjola et al., 2010). The development of the high-speed technology has been, first of all, the development of electrical machines, frequency converters, high specification materials and development of manufacturing methodology of the applications. (Gerada et al., 2010).

The advantage of the high-speed technology is the higher power density and the smaller size in comparison with a conventional drives. The same power rating is established with smaller and lighter equipments. Additionally there is no need to transform the speed between drive and application by a gearbox, which means that there does not exist those power losses. (Kolondzovski, 2010).

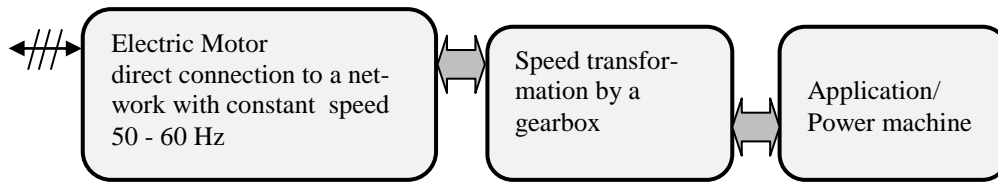


Figure 1a: Conventional drive concept

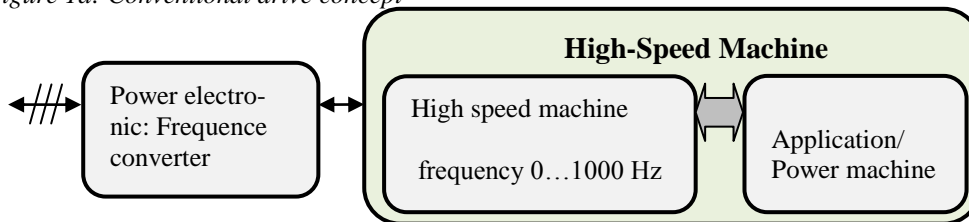


Figure 1b: The high-speed drive concept.

The conceptual schematic of the conventional drive is shown in Fig.1a, where the gearbox transforms the rotating speed between the drive and the application. In Fig.1b the gearbox is replaced by a power electrical converter. The drive and the application are connected on a common shaft and the speed of this rotor can easily be controlled by a frequency converter. In a typical high-speed application, like turbo compressors or turbo generators, equipments can operate with a high efficiency in variable load conditions using speed control. Inherently it is a more energy efficient way compared to throttle valve control of the flow. The speed control produces less power losses and provides a higher efficiency. High-speed applications have been adapted to the distributed energy production, industry compressors, pumps and cooling machines. (Larjola, 1986), (Larjola et al., 1991), (Jokinen et al., 1998), (Kaikko et al., 2003), (Backman et al., 2004), (Reunanen et al., 2005), (Larjola, 2011), (Turunen-Saaresti et al., 2010), (Tang et al., 2008).

As the power densities increase, also the loss densities increase, which leads to elevated material temperatures. At high rotating speeds mechanical strains increases as well; centrifugal forces have a proportion on the speed of power of two. Residual unbalance can cause lateral forces to the shaft of rotor, which can lead to uncontrollable vibrations and damage the rotor. It is possible to determine the effects of unwanted vibrations using rotor dynamics theory in the rotor dimensioning. Designing of high-speed machines require accurate dimensioning and sophisticated calculation methods, because it operates at extreme conditions with weakened material properties.

In high-speed machines there are no power losses from a gearbox system, but mechanical and electrical losses may increase. In bearings they are generated as gas friction losses and in the electric machine as electrical losses caused by the high frequency of the stator flux variation. The development of gas and magnet bearings has decreased the bearing losses. The high power density of the electric machine and the rotor composes challenges to the cooling demand because of the increase in the core losses and decrease with the cooling areas. However, the continued development of material properties improves the situation.

LITERATURE REVIEW

In a design of a high efficient high-speed machine rotor with good mechanical properties, it is important to base the work on multi physical approaches, where the electromagnetic, the mechanical and the thermal aspects are considered at the same time. Optimum solutions where various physical factors are taken into account needs to exploit software that can solve simultaneous tasks. (Gerada et al., 2010).

Not only the high-speed drive but also the application needs to be considered as a potential object of development in combination. The economical factors set the limits for commercial technical solutions. It is not only opportunities of technology that dictates the solution to be accomplished but also commercial circumstances, and the ultimate outcome is a compromise of these two factors. This multilateral relationship is depicted in Figure 2, (Gerada et al., 2010).

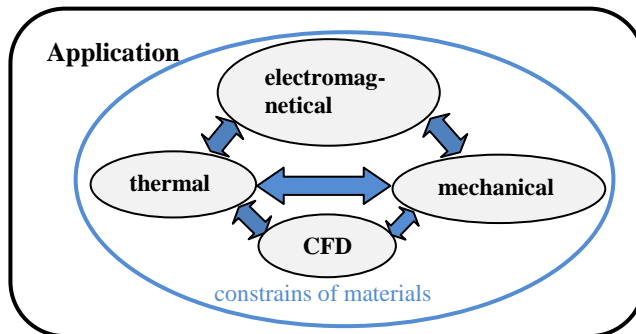


Figure 2: Relationships of various branch of science and constrains of designing a high-speed equipment.

The design of a high-speed machine considers as the main aspect the high power density, when the active cooling of the electric machine is highlighted. As a result of a high rotating speed of a rotor, centrifugal forces increase and the structure of the shaft must carry the loads and have an adequate rigidity when the rated operating point is below the speed of the first critical bending. As a result of a high supply frequency, the power losses increase in a stator which increases the necessity of cooling. A large cooling air flow through the air-gap increases the airflow losses, which consist of two factors: 1) air friction losses that are independent of the mass of the air and are proportional to the cube of the speed 2) the amount of mass of air dependent factor that is proportional to the square of the speed. Another reason for a rotor temperature rise is the asynchronous mmf-waves in the air-gap. To minimize the power losses, that include stator and rotor core losses as well as the resistive losses, the choice of suitable materials is essential for different parts of the rotor. The essential material properties include good electrical and mechanical properties at elevated temperature conditions. (Aglén et al., 2003), (Saari, 1998), (Soong et al., 2000), (Wang et al., 2008)

By and large, eddy current losses in permanent magnet machines are diminutive compared to induction machines. Eddy currents are generated on the rotor and magnets surface due to harmonics of current. Losses in the rotor core are negligible in permanent machines, because the induction current is not present. Eddy current losses can be the cause of time harmonics and space harmonics. Time harmonics can be cure by filtering the signal to get more pure sinusoidal waveform. Space harmonics are a consequence of the stator slots and can be reduced by making slots more closed by filling them and overlapping the stator winding (Arkkio et al., 2005), (Cho et al., 2006), (Li et al., 2010), (Wang et al., 2008).

Rotor losses in induction machines are more significant due to the currents in the rotor core. Therefore, the rotor materials should have optimal magnetic and electrical properties. Rotors of induction machines have not sensitive parts for mechanical and thermal loads like permanent magnets in synchronous machines. In general induction machines are more reliable than permanent magnet machines, but the synchronous machines are more power efficient. (Gerada et al., 2008), (Soong et al., 2000).

The design process of a high-speed turbo-machinery is expressed as a flow chart (Fig. 3), which includes the route from the phase of concept design to the phase of prototype production. In the chart from various phases of the process are expressed, including their contents and mutual relationships, information flows and feed-back. The optimal solution requires usually from two to three cycles of iteration.

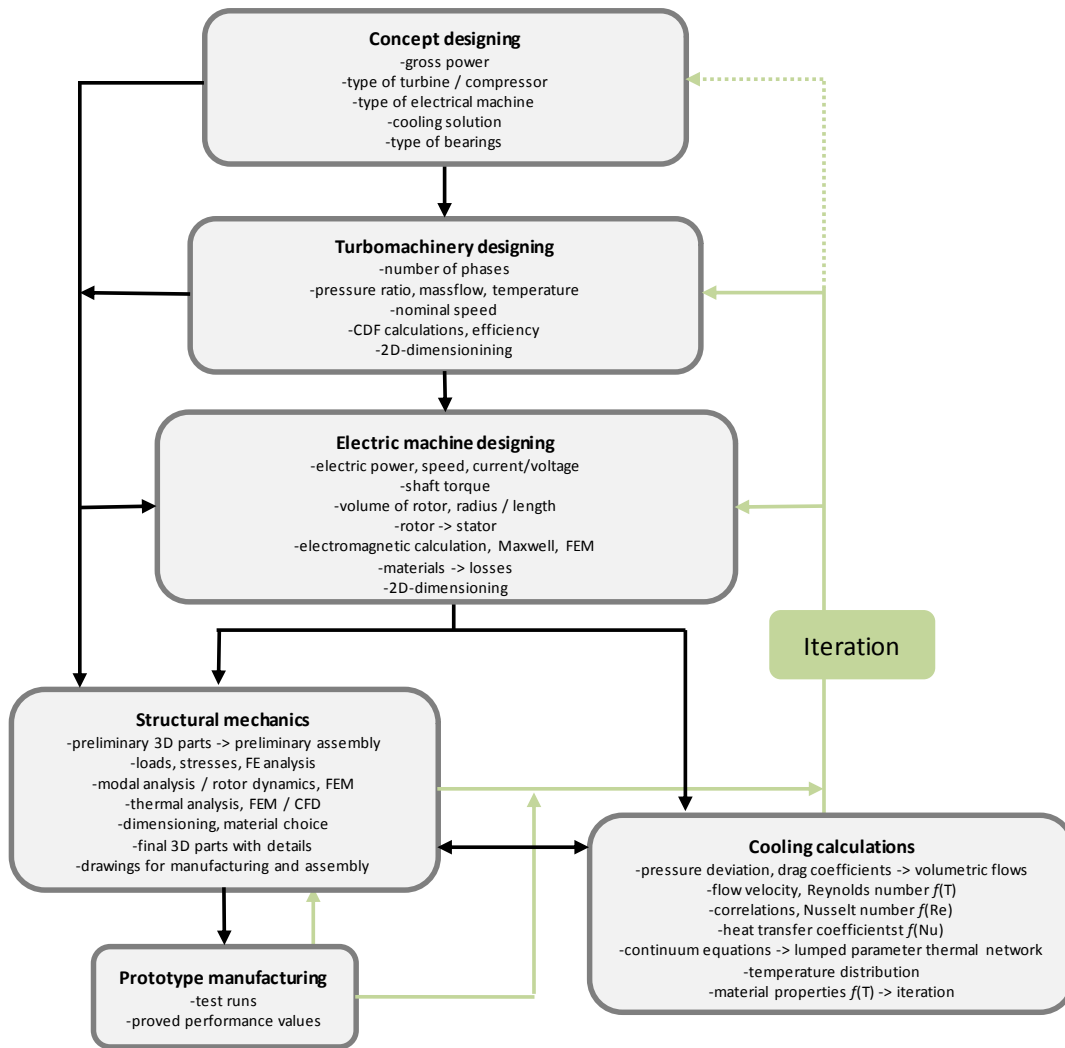


Figure 3: Process flow of the design of turbo-machinery applications.

DIMENSIONING OF THE HIGH-SPEED MACHINE

Governing equations for high speed machines are expressed to a) size the electric machine, b) to calculate the losses in the cooling flow, c) to calculate the equations of heat generation, d) to calculate the mechanical stresses of the rotor and e) to calculate the natural frequencies of the rotor.

The cooling is an essential role in high-speed machines because of high power density. At the same time increased gas flow friction losses complicate the cooling. The sort of heat transfer equations are performed of a heat transfer of gas flow governing equations, also heat transfer coefficients in contacts between parts, heat transfer coefficient as a function of contact pressure.

Dimensioning of the electric machine

The rotor synchronous speed n_s is defined with Eq. (1)

$$n_s = \frac{f}{p} \quad (1)$$

The rotor volume and the power of the electric motor are linked in Eq. (2)

$$V = \frac{\pi P p}{4 C f} \quad (2)$$

where C is the machine dependent factor in Eq. (3)

$$C = \frac{\pi^2}{\sqrt{2}} k_w A_c \hat{B}_\delta \quad (3)$$

As the mass of the rotor m_r is proportional to the volume V , we can derive Eq. (4)

$$m \sim m_r \sim \frac{pP}{f A_c \hat{B}_\delta} \quad (4)$$

With the constant parameters A_c and \hat{B}_δ , the mass of the rotor is inversely proportional to the synchronous frequency f , and proportional to the number of pole pairs p and power P . (Jokinen and Luomi, 1988).

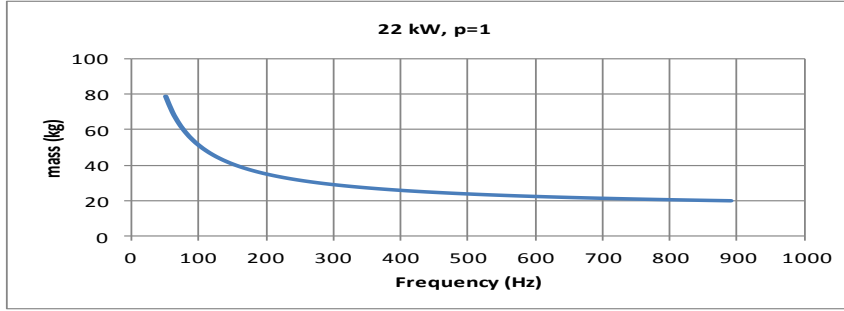


Figure 4: The effect of the nominal frequency of the electric machine to the mass of the machine (without the frame). Induction machine with a number of pole pairs of 1 and power of 22 kW.

The proportionality to the iron losses are presented in Eq. (5)

$$P_{Fe} \sim \hat{B}_\delta^2 f^2 D^3 \sim \hat{B}_\delta^2 n_s^2 D^3 \quad (5)$$

Temperature rise is proportional to the area of the cooling. The temperature increase is linear as the iron losses are constant

$$\frac{P_{Fe}}{A} \sim \frac{\hat{B}_\delta^2}{D} \quad (6)$$

Cooling flow losses

Channeling an air flow through the air gap of a stator and a rotor is a common way to cool these parts. Rotating surface of the rotor with a high speed, on the one hand accelerate air flow to tangential movement and on the other hand there exist a friction between air and the surface. Cooling air flow losses are expressed in equations (7) – (9).

Regarding of an air friction losses, a high-speed rotor consist of a cylinder surface, which is surrounded by the stator of the electric machine, which forms an annular channel between two nested cylinders. In addition air friction losses at the ends of a cylinder. The calculation of losses can be divided in two parts according Fig. 5a.

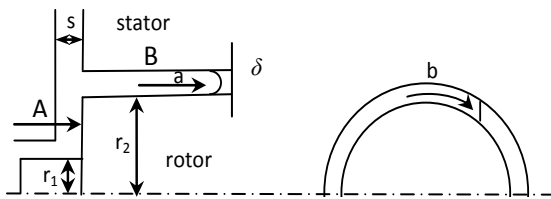


Figure 5a: Air friction losses division: A) rotating disc friction losses at the ends of rotor. B) losses from air flow in the air gap δ can be divided a) air friction losses, b) flow losses that depend of amount of tangential acceleration of the mass flow.

Rotating cylinder (a) gas friction losses (Saari, 1998) P can be expressed:

$$P = k_1 C_f \pi r \omega^3 r^4 l \quad (7)$$

where k_1 a roughness coefficient (1 for smooth surface) and the friction coefficient C_f can be obtained from Fig. 5b_{left}.

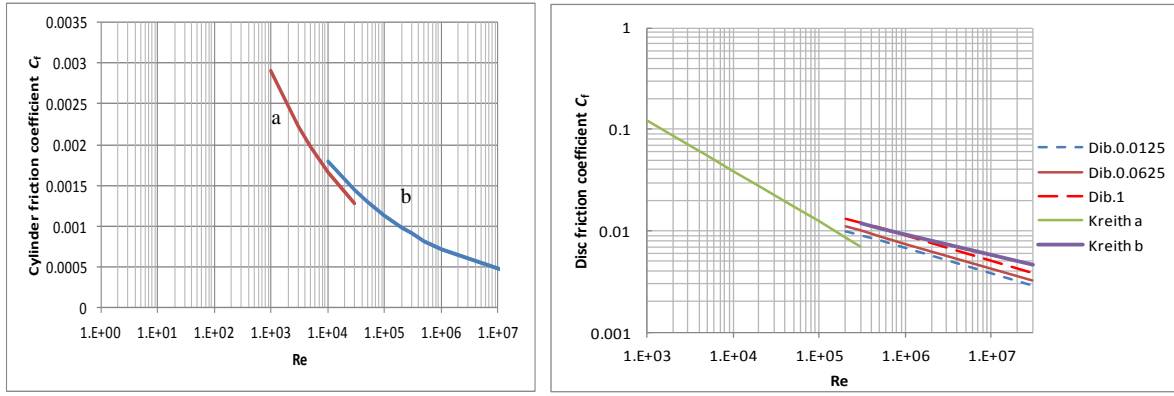


Figure 5b: (Left) Friction coefficients of a rotating cylinder, line a according Saari (1998) eq.11 and line b eq.14b, where $\delta=2\text{mm}$ and $r_1=68\text{mm}$. (Right) Friction coefficients of a disc according Saari (1998)(Kreith a, b) eq. 17a, b. Dib.0.0125-1 denotes s/r_2 relation (Fig5a) according Larjola(2006.) Both graphs as a function of the Reynolds number.

The friction losses of a rotating disc (A) are estimated with the equation of the disc flow (Eq. 8), where the result includes both ends of the rotor (Saari, 1998).

$$P = 0.5 \cdot C_f \rho \omega^3 (r_2^5 - r_1^5) \quad (8)$$

where, r_1 and r_2 are the inner and outer radii of the end disc. Friction coefficient C_f is obtained from the Fig. 5b_{right}.

Mass flow dependent power losses P (b) on the rotor surface in the air gap, with open stator slots, where the flow is in axial direction, can be get:

$$P = k_2 q_m u_1^2 \quad (9)$$

where k_2 is a velocity coefficient, q_m is a through-flow mass, u_1 is the peripheral speed. A typical value for k_2 is 0.15. (Saari et al., 2002).

Thermo-analytical equations

The Nusselt number defines the heat transfer properties of the flow in air gap compared with a pure heat conductance. For a rotating cylinder (stator-rotor air gap) the Nusselt number (Nu) is: (Larjola and Kuosa, 2004).

$$\text{Nu} = 0.0214(\text{Re}^{0.8} - 100)\text{Pr}^{0.4} \left[1 + \left(\frac{d_h}{L} \right)^{0.66} \right] \quad (10)$$

In Eq. (10) d_h is a hydraulic diameter, Pr is a Prandtl number, Re is a Reynolds number and L is the length of rotor in air gap. The heat transfer coefficient h in the air gap is

$$h = \frac{\text{Nu}\lambda}{d_h} \quad (11)$$

where h is a heat transfer coefficient, λ is a heat conductance coefficient. The heat transfer coefficient h elsewhere than in air gap, like on flat surfaces, can be got by a case sensitive equations (see VDI-Wärmeatlas), and the Nusselt number is calculated according to the following equation.

$$\text{Nu} = 0.037\text{Re}^{0.8}\text{Pr}^{0.4} \quad (12)$$

Contact pressure in joints

A heat transfer properties between the parts in contact are defined by a contact pressure, a properties of materials (steel-aluminum) and a properties of surface roughness (1 - 2 μm). Although the heat transfer coefficient h depends of the properties of the materials, the chart (Fig. 6) can be expressed according to values of different sources. (Fletcher, 1988).

As mentioned above there are points in a high-speed applications, where cylinder surfaces are connected together with a tight fit: For instance an impeller to the shaft. The equations for this kind

of junctions can be found from reference Juuma (2001). In the FE analysis the contact pressure can be obtained directly from the results.

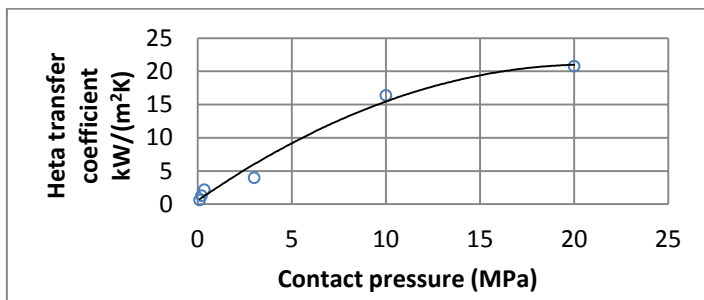


Figure 6: A heat transfer coefficient as a function of a contact pressure.

EXAMPLE OF A PROPER DESIGN: TURBOCOMPRESSOR

The example of this project consists of a turbomachine with a radial compressor, an axial turbine and an electric machine. The electric machine is an asynchronous induction machine.

The optimum nominal speed of the turbomachine is 28000 rpm. The rotor structure must allow also operation speeds up to 31500 rpm, if the nominal power is briefly exceeded. The rotor will operate at over speed circumstances, for instance in a situation where the electrical load is switched off or the load of the compressor suddenly disappears. The rotor structure must tolerate generator rushes. The structure of the induction machine is expressed in figure 7.

There are many reasons for speed limits, for instance the fittings of compressor and turbine wheels to the shaft may be loosened. This can lead to an unbalance of the shaft exceeding the permitted limits. Also the fits of the bandaging of the end rings of the rotor squirrel cage may come loose.

At the design speed of 28 000 rpm the calculated values of various parts are: a) the power consumed by the compressor is 716 kW, b) the power generated from the turbine is 986 kW, c) the mechanical losses are 28 kW and the electrical losses are 8 kW and the net electric power is 234 kW.

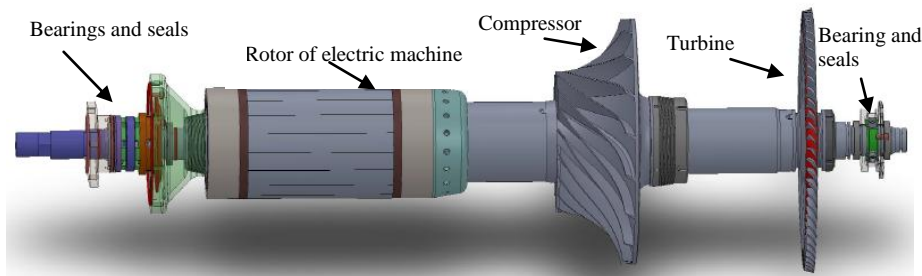


Figure 7: A rotor structure of an induction machine.

The structure of the rotor of asynchronous machine

The alternating current in the stator of an induction machine induces current to flow in the rotor bars and consequently a magnetic field and mmf (magneto motive force) that force the rotor to follow the rotating field of the stator at the line frequency. The total losses in the rotor consist of winding losses and core losses. The winding losses originate from fundamental frequency, space harmonics and time harmonics. The core losses originate solely from space and time harmonics.

Fig. 8 presents the structure of the rotor squirrel cage. All the parts fixed on the rotor experience the centrifugal force, which expands the rings outwards in the radial direction. The fits are easily loosened as the end rings are manufactured of a copper alloy that has a high density to elastic deformation. For instance, the density of an alloy CuCr1Zr is 8900 kg/m^3 , the modulus of elasticity is 110 – 130 GPa and the yield strength is 440 MPa. It is compulsory to use a bandage with a stringent

fit. The usage of high strength steel does not have to have any special electrical properties, but a non magnetic material is an advantage.

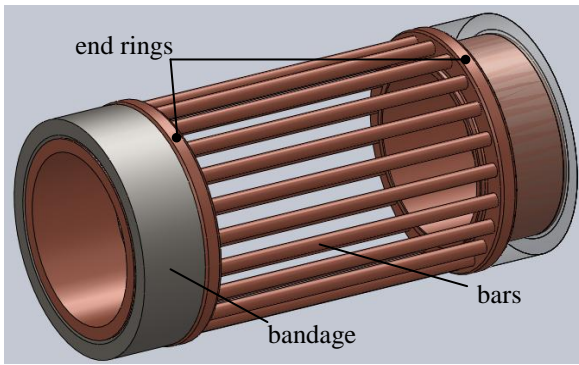


Figure 8: The rotor structure of an induction machine. A copper cage assembly with copper bars $d = 8 \text{ mm}$ (22 pcs), end rings and bandages.

Temperatures of rotor and conduits

The dissipation in the rotor core of an induction machines leads to a temperature rise. Especially on a thin section area of the outer surface of the rotor comprises about 60 % of total losses and the remaining losses are produced in the core. The copper losses in the end rings and bars are small, only 6 % of total losses, Fig. 9 (compare to Fig. 8).

Figure 10 a - b presents the temperature distribution of the rotor core and surface. Fig.10a depicts the case no cooling air flow through the holes and Fig.10b the case air flows through the holes.

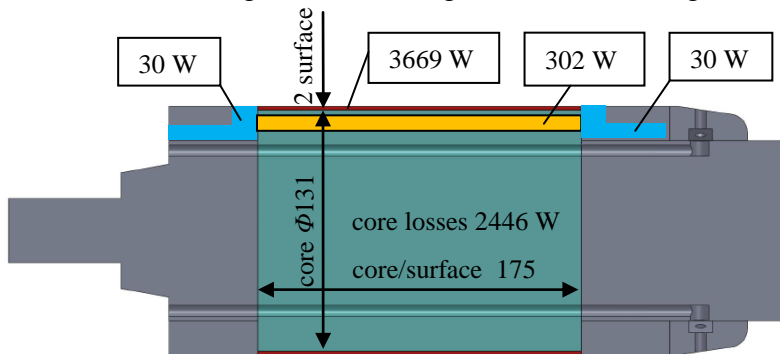
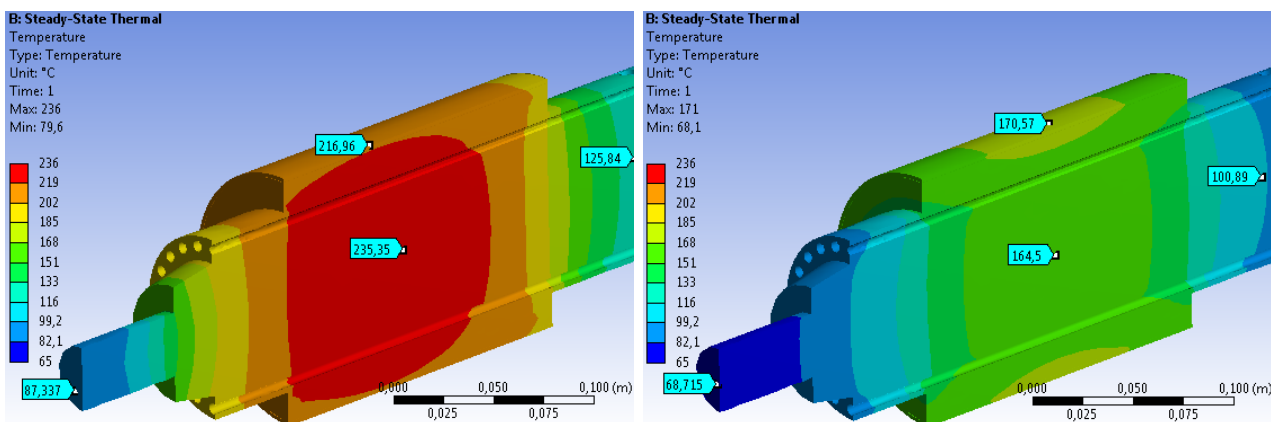


Figure 9: Dimensioning of a rotor of an electric machine. In the rotor core losses are 2446 W and on the surface 3669 W. There are 22 pcs round bars with total losses of 302 W. The core volume is 2.25 dm^3 and the power density is 1.22 kW/dm^3 . The rotor surface thickness is 2 mm, the volume is 0.15 dm^3 and the power density is 25.1 kW/dm^3 . The power losses on the end rings are 60 W in total.



a) Figure 10: Temperature distribution ($^{\circ}\text{C}$) of the rotor an induction machine. a) No cooling flow through the rotor holes. b) A cooling flow of 107.6 g/s through the rotor holes. Heat transfer coefficient in the air gap is $980.8 \text{ W/(m}^2\text{K)}$ and the cooling flow is 37.9 g/s are the same in both cases (bandages, bars and end rings are not visible).

Stresses of turbo impellers and the shaft

In the initial phase of the design of the turbocompressor (Fig. 7), the rotating speed of the rotor is chosen so that both the compressor and the turbine efficiencies are as good as possible. However, the speed has to be below the first bending mode of the rotor and the stresses have to remain under the yielding limit. Both the compressor and the turbine impellers are fixed to the shaft with a tight interference fit. There turbine impeller assembly is more demanding of the two impeller rotors.

The fixing of the turbine impeller onto the rotor shaft must remain secured in all conditions to prevent any unbalance of the rotating shaft. The joints must have an adequately tight fit to remain gapless in all conditions and rotating speeds. The centrifugal force lowers the contact pressure between the shaft and the impeller, so there must remain sufficient contact pressure as the rotating speed increases. However, the fits cannot be too tight regarding the limit of the yield strength. The tightness of the fit is at maximum when assembled to the shaft, but is loosened as the rotating speed increases. There should remain at least some interference fit in overspeed situations, as well.

The maximum stress on the shaft at the assembly stage (0 rpm) is about 650 MPa, Fig. 11a. Figure 11b shows the remaining contact pressure on the both side areas of the turbine hub and is 80 – 90 MPa. Figure 11c shows the stresses on the impeller hub, being about 850 MPa. In the middle of the disc, the maximum stress is about 480 MPa at a rotating speed 28500 rpm. The disc and hub of the wheel must have a certain configuration in order to achieve even stress distribution. The material of turbine wheel is a special-steel Orvar Supreme ultimately hardened to 1600 MPa.

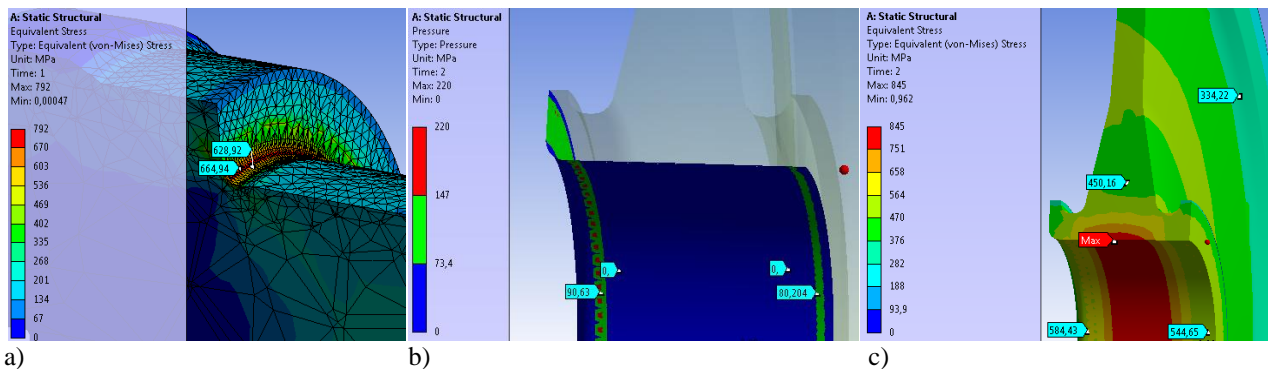


Figure 11: Assembling a turbine wheel to the shaft, a) stress distribution of the shaft, b) contact pressure of the hub as a nominal speed c) stresses at the hub as a nominal speed 28500 rpm.

One way to allow higher rotating speed is to make the joint wider. This however increases the length of the shaft and consequently lowers the natural frequency of the first bending mode. Another way may be to change the principle of fixing parts in the conjunction. In Fig. 12 can be seen the stresses in the middle of the disc and in the hub as a function of the speed. At a rotating speed of 31500 rpm and higher it is quite obvious to lose a contact between parts.

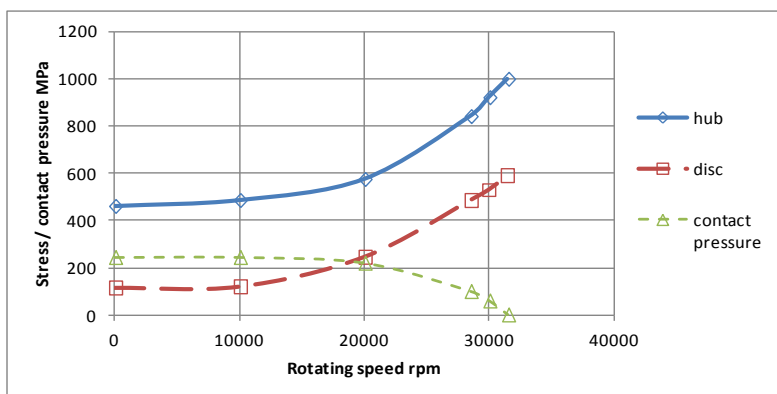


Figure 12: Stresses in the impeller and the contact pressure in the conjunction.

CONCLUSIONS

This research considers rotating high-speed machines, which are the combination of an electric machine and a turbomachine, which have a common rotor. The main targets of the development are to reduce the losses and improve the cooling and the bearing arrangements, including the rotor stability. The first critical speed of bending of rotor can be exceeded and operated at overcritical speed, but this requires an expensive three plane balancing and complex control system. Thus it is usually economically more feasible to use subcritical rotors. Decreasing of losses in stator and rotor of electric machine has been in good progress, mainly because of development of new, finite element based computation programs, programs combining different technologies and increase of computation capacity. Properties of materials used in high-speed machines are also very important. They should meet special requirements in electromagnetic, physical, thermodynamical and strength properties.

A turbo-compressor is considered as an example, which is combination of electric machine, compressor and turbine. It is used in a combustion engine in order to improve its performance. The temperature distribution and cooling of this rotor is considered. In turbine it is considered the strength of interference fit used. At high speed this fit will loosen, but some interference should remain also at over speed, in order to avoid unbalance. The safe margin of the interference fit can be increased by making the length of the fit slightly more wide.

This research makes clear, that normal analytical equations used independently are not sufficient in design of high-speed rotors with high power density. It is necessary to use programs, which combine equations of different branches of technology. These programs are often based on finite element method. Taking in account both electromechanical, thermo-dynamical, rotor dynamical and strength aspects simultaneously gives nearly optimum solution in a high-speed rotor design.

ACKNOWLEDGEMENTS

The material for this study was obtained in several research projects conducted in Lappeenranta University of Technology during 2006 -2012. Authors would like to thank the Tekes - the Finnish Funding Agency for Technology and private companies involved in these projects for supporting this work. Also, they want to thank Lic. Tech. Honkatukia and Doctors Nerg, Grönman, Sallinen and Punnonen for giving valuable advice.

REFERENCES

- Aglén, O., Andersson, Å. 2003. Thermal analysis of a high-speed generator. *Proceedings of the 38th IAS annual meeting*, Vol.1, 12-16 October 2003, pp. 547-554.
- Arkkio, A., Jokinen, T., Lantto, E. 2005. Induction and permanent-magnet synchronous machines for high-speed applications. *Proceedings of the 8th International Conference on Electrical Machines and Systems - ICEMS 2005*, Vol. 2, 27-29 September 2005, pp. 871-876.
- Backman, J., Reunanen, A., Esa, H., Punnonen, P., Honkatukia, J., Larjola, J. 2004. Concept Design of a Solid Oxide Fuel Cell Gas Turbine, HPC 2004 – 3rd International Conference on Heat Powered Cycles. Larnaca, Cyprus October 11 - 13, 2004, 7 p., CD, ISBN 01874418353.
- Cho, H.W., Jang, S.M., Choi, S.K. 2006. A design approach to reduce rotor losses in high-speed permanent magnet machine for turbo-compressor. *IEEE Transactions on Magnetics*, Vol. 42, No. 10, October 2006, pp. 3521-3523.
- Dibelius G., Radtke F., Zierman M.1984. Experiments of friction, velocity and pressure distribution of rotating disc. Chapter in: Heat and mass transfer in rotating machinery, edited by Metzger and Afgan. Springer-Verlag, Berlin.
- Gerada, D., Mebarki, A., Brown, L.N., Gerada, C. 2010. Optimal Split Ratio for High Speed Induction Machines. *IEEE Energy Conversion Congress and Exposition (ECCE)*, 12 – 16 Sept. 2010, pp. 10 - 16.
- Kaikko, J., Backman, J., Larjola, J., Sarkomaa, P. 2003. Performance comparison between single and multiple generator type variable-speed micro turbine with intercooling, reheating and recu-

peration, The 5th European Conference on Turbomachinery - Fluid Dynamics and Thermodynamics, Prague, Czech Republic, March 18-21, 2003, pp. 1145-1156.

Kolondzovski, Z. 2010. Thermal and Mechanical Analyses of High-Speed Permanent-Magnet Electrical Machines. ISBN 978-952-60-3280-1 (PDF) Monikko Oy, Espoo, 2010, 94 p. (Doctoral thesis).

Larjola, J. 1986. High Speed Turbomachinery and its application in the conversion of energy. ASME Winter Annual meeting, Anaheim, USA, December 7-12, 1986, ASME publ. 86-WA/FE-4, 1986.

Larjola, J. 2006. Pyörivän kiekon kitka. Lecture notes, Boundary layer theory, Lappeenranta 2006.

Larjola, J. 2011. Organic Rankine cycle (ORC) based waste heat / waste fuel recovery systems for small CHP applications, Small- and micro-combined heat and power (CHP) systems, Advanced design, performance, materials and applications., 2011, pp. 206-232, ISBN 978-1-84569- 795-2, Woodhead Publishing Limited, Oxford.

Li, W., Wang, J., Zhang, X., Kou, B. 2008. Loss Calculation and Thermal Analysis of Three Modes of Retaining Sleeves for High-Speed PM Generators. 978-1-4244-7062-4/10/\$26.00 ©2010 IEEE.

Reunanen, A. and Larjola, J. 2005. Radial Forces in a Centrifugal Compressor; Experimental Investigation by Using Magnetic Bearings and Static Pressure Distribution., Journal of Thermal Science, 2005, vol. 14, nro. 1, pp. 1-9, ISSN 1003-2169.

Saari, E. 2012. Thermodynamical and mechanical modelling analysis of high-speed turbomachine rotors. (in Finnish) Acta Universitatis Lappeenrantaensis, diss., Lappeenranta, 121 p.

Saari, J. 1998. Thermal analysis of high-speed induction machines. *Acta Polytechnica Scandinavica, Electrical Engineering Series*, No. 90, Espoo, 73 p. (Doctoral thesis).

Saari, J., Sallinen, P., Larjola, L. 2002. Evaluation of frictional and gas flow losses in high-speed electrical machines. Research Report EN A-52, Lappeenrannan teknillinen korkeakoulu ISBN 951-764-628-3, ISSN 0785-823X.

Soong, W. L., Kliman, G. B., Johnson, R. N., White, R. A., and Miller, J. E., 2000. Novel High-Speed Induction Motor for a Commercial Centrifugal Compressor. *IEEE Transactions on Industry Applications*, Vol. 36, No. 3, May/June 2000.

Tang J., Turunen-Saaresti T., Larjola J. 2008. Use of partial shrouded impeller in a small centrifugal compressor. Journal of Thermal Science in Vol. 17 No. 1. 2008.

Turunen-Saaresti T., Røyttä P., Honkatukia J., Backman J. 2010. Predicting the off-design range and performance of refrigeration cycle with two-stage centrifugal compressor and flash intercooler. International Journal of Refrigeration, vol. 33 Issue 6, pp. 1152- 1160, September 2010.

VDI-Wärmeatlas; Berechnungsblätter für den Wärmeübergang. VDI-Verlag GmbH, Düsseldorf 1984.

Wang, J., Wang, F., Kong, X. 2008. Losses and thermal analysis of high speed PM machine. *Proceedings of the Joint International Conference on Power System Technology and IEEE Power India Conference – POWECON'08*, 12-15 October 2008, 5 p.